

# Cluster of Clusters: A Modular Approach to Large Metal Clusters. Structural Characterization of a 38-Atom Cluster [(*p*-Tol<sub>3</sub>P)<sub>12</sub>Au<sub>18</sub>Ag<sub>20</sub>Cl<sub>14</sub>] Based on Vertex-Sharing Triicosahedra

Boon K. Teo,\* Hong Zhang, and Xiaobo Shi

Contribution from the Department of Chemistry, University of Illinois at Chicago, Chicago, Illinois 60680. Received November 27, 1989

**Abstract:** The crystal and molecular structure of a 38-atom metal cluster, (*p*-Tol<sub>3</sub>P)<sub>12</sub>Au<sub>18</sub>Ag<sub>20</sub>Cl<sub>14</sub> (**1**), has been determined by single-crystal X-ray crystallography. The cluster (*p*-Tol<sub>3</sub>P)<sub>12</sub>Au<sub>18</sub>Ag<sub>20</sub>Cl<sub>14</sub>·42EtOH crystallizes in a triclinic unit cell of *P*-1 space group with lattice parameters *a* = 23.094 (11) Å, *b* = 31.950 (17) Å, *c* = 34.178 (17) Å, α = 112.76 (4)°, β = 90.04 (3)°, γ = 97.92 (3)°, and *Z* = 2. The structure was refined to *R*<sub>1</sub> = 10.1%, *R*<sub>2</sub> = 11.8% for 8150 independent reflections with *I* > 3σ(*I*). The metal framework of **1** can be described as three 13-atom centered icosahedra sharing three vertices in a triangular array plus two capping Ag atoms on the pseudo-3-fold axis. As such, it belongs to a novel series of high-nuclearity Au-Ag clusters whose structures are based on vertex-sharing (centered) icosahedra. Empirical structural rules for these Au-Ag supraclusters are developed. The structural systematics of this new class of supraclusters led to the concept of "cluster of clusters", which is useful in the design, preparation, and characterization of large metal clusters of increasingly high nuclearity via vertex-, edge-, and face-sharing and/or close packing of smaller cluster units as building blocks (viz., a modular approach to large clusters). Simple electron counting of this and related clusters based on a cluster of clusters (C<sup>2</sup>) model is also discussed in order to rationalize the observed structural parameters and the electronic requirements.

## (I) Introduction

Generally speaking, there are two broad categories of highly symmetrical high-nuclearity metal clusters: the  $\nu_n$  polyhedral clusters and the  $s_n$  supraclusters. A  $\nu_n$  polyhedral cluster is defined as a cluster with (*n* + 1) atoms on each edge of the polyhedron.<sup>1</sup> Chart I portrays the early members of the  $\nu_n$  icosahedral clusters (Mackay<sup>2a</sup> sequence). The magic numbers, defined as the nuclearity (number of atoms) of a cluster, are given in parentheses. These magic numbers represent structurally stable, often closed-shell, configurations of atoms in a cluster and can be observed experimentally. For example, adiabatic jet expansion of inert gas (e.g., Xe) produces van der Waals clusters following the sequence of magic numbers<sup>2b</sup> 1, 13, 55, 147, ...

An  $s_n$  supracluster is defined as a cluster of *n* smaller cluster units fused together via vertex-, edge- or face-sharing.<sup>3,4a</sup> Chart II illustrates the early members of supraclusters based on vertex-sharing centered icosahedral cluster units of 13 atoms. Since these supraclusters,  $s_n$ , are made up of smaller cluster units, they are referred to as a *cluster of clusters*.<sup>3,4</sup>

Gold cluster chemistry dates back to the early 1970s with the report of the reduction of (Ph<sub>3</sub>P)AuI by NaBH<sub>4</sub> to produce (Ph<sub>3</sub>P)<sub>7</sub>Au<sub>11</sub>I<sub>3</sub>.<sup>5</sup> Recent developments<sup>6</sup> in gold phosphine chemistry have produced a novel series of gold clusters up to Au<sub>13</sub>, which has a centered icosahedral structure [see  $\nu_1(13)$  of Chart I].<sup>1</sup> Most, but not all, of the structures of the Au<sub>*n*</sub> (*n* < 13) clusters can be considered as based on this centered icosahedral structure with

Chart I.  $\nu_n$  Polyhedral Clusters

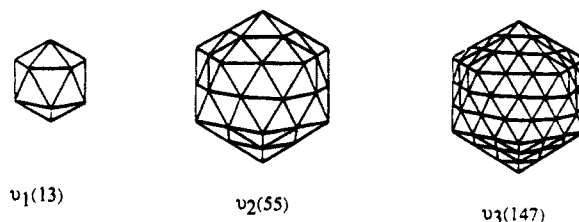
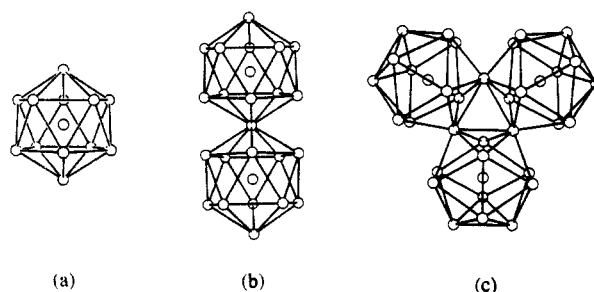


Chart II.  $s_n$  Supraclusters: (a)  $s_1(13)$  (b)  $s_2(25)$  (c)  $s_3(36)$



(13 - *n*) missing vertices. In contrast, similar reactions with the silver analogues produced only insoluble materials.<sup>7</sup>

It occurred to us in 1984 that a combination of Au and Ag might be a fruitful way to produce large metal alloy clusters. This idea resulted in the isolation and structural characterization a 25-atom cluster.<sup>8</sup> Our recent work gives rise to a number of new clusters including a new 25-atom [(*p*-Tol<sub>3</sub>P)<sub>10</sub>Au<sub>13</sub>Ag<sub>12</sub>Br<sub>8</sub>](PF<sub>6</sub>),<sup>9</sup> a 37-atom cluster [(*p*-Tol<sub>3</sub>P)<sub>12</sub>Au<sub>18</sub>Ag<sub>19</sub>Br<sub>11</sub>](AsF<sub>6</sub>),<sup>3a</sup> and the title compound, the 38-atom cluster [(*p*-Tol<sub>3</sub>P)<sub>12</sub>Au<sub>18</sub>Ag<sub>20</sub>Cl<sub>14</sub>]. It turns out that the 25-, 37-, and 38-atom clusters follow (or are based on) the magic numbers of the supracluster sequence  $s_n$  depicted in Chart II. In other words, the 25 (Au<sub>13</sub>Ag<sub>12</sub>), 37 (Au<sub>18</sub>Ag<sub>19</sub>), and 38 (Au<sub>18</sub>Ag<sub>20</sub>) metal atoms clusters can all be considered as being built from 13-atom centered icosahedral cluster units. Thus, the 25-atom cluster can be described as two ico-

(1) Teo, B. K.; Sloane, N. J. A. *Inorg. Chem.* **1985**, *24*, 4545.  
 (2) (a) Mackay, A. D. *Acta Crystallogr.* **1962**, *15*, 916. (b) Eicht, O.; Sattler, K.; Recknagel, E. *Phys. Rev. Lett.* **1981**, *47*, 1121.  
 (3) (a) Teo, B. K.; Hong, M. C.; Zhang, H.; Huang, D. B. *Angew. Chem., Int. Ed. Engl.* **1987**, *26*, 897. (b) Teo, B. K.; Hong, M.; Zhang, H.; Huang, D.; Shi, X. *J. Chem. Soc., Chem. Commun.* **1988**, 204.  
 (4) (a) Teo, B. K.; Zhang, H. *Inorg. Chem.* **1988**, *27*, 414. (b) Teo, B. K.; Zhang, H. *Inorg. Chim. Acta* **1988**, *144*, 173. (c) Teo, B. K. *Polyhedron* **1988**, *7*, 2317.  
 (5) (a) Malatesta, L.; Naldini, L.; Simonetta, G.; Cariati, F. *J. Chem. Soc., Chem. Commun.* **1965**, 212. (b) McPartlin, M.; Mason, R. *J. Chem. Soc., Chem. Commun.* **1969**, 334. (c) Cariati, F.; Naldini, L. *Inorg. Chim. Acta* **1971**, *5*, 172.  
 (6) (a) Steggerda, J. J.; Bour, J. J.; van der Velden, J. W. A. *Recl. Trav. Chim. Pays-Bas* **1982**, *101*, 164. (b) Hall, K. P.; Mingos, D. M. P. *Prog. Inorg. Chem.* **1985**, 237. (c) Puddephatt, R. J. *The Chemistry of Gold*; Elsevier: New York, 1978.

(7) Teo, B. K.; Zhang, H., to be published.  
 (8) Teo, B. K.; Keating, K. *J. Am. Chem. Soc.* **1984**, *106*, 2224.  
 (9) Teo, B. K.; Zhang, H.; Shi, X. *Inorg. Chem.* **1990**, *29*, 2083.

**Table I.** Summary of Crystal Data, Collection and Reduction of X-ray Data, and Solution and Refinement of Structure of (*p*-Tol<sub>3</sub>P)<sub>12</sub>Au<sub>18</sub>Ag<sub>20</sub>Cl<sub>14</sub>·42EtOH (1)

A. Crystal Data	
formula	( <i>p</i> -Tol <sub>3</sub> P) <sub>12</sub> Au <sub>18</sub> Ag <sub>20</sub> Cl <sub>14</sub> ·42EtOH
crystal color	dark red
crystal shape	prism
crystal size, mm <sup>3</sup>	0.1 × 0.1 × 0.05
cell parameters (errors)	
<i>a</i> , Å	23.094 (11)
<i>b</i> , Å	31.950 (17)
<i>c</i> , Å	34.178 (17)
$\alpha$ , deg	112.76 (4)
$\beta$ , deg	90.04 (3)
$\gamma$ , deg	97.92 (3)
cell volume, Å <sup>3</sup>	22992.3 (7)
<i>Z</i>	2
Laue symmetry	triclinic
space group	<i>P</i> -1
systematic absences	no conditions
equivalent positions	- <i>x</i> , - <i>y</i> , - <i>z</i>
B. Collection and Reduction of X-ray Diffraction Data	
diffractometer	Enraf-Nonius CAD4
radiation	Mo K $\alpha$
wavelength, Å	0.7107
temperature, °C	23 ± 2
scan technique	$\omega/2\theta$
scan rate (limits), deg/min	4–16
scan range, deg	(0.6 + 0.35 tan $\theta$ )
no./freq of std reflns	3/200
2 $\theta$ limits, deg	2 < 2 $\theta$ < 46
cutoff of obsd data	3 $\sigma(I)$
no. of unique data <sup>a</sup>	64 687
octants	$\pm h, \pm k, \pm l$
linear absorptn coeff, cm <sup>-1</sup>	68.8
range of transmission	81.46–99.84%
C. Solution and Refinement	
technique of solution	direct method
method of refinement	full-matrix least-squares <sup>b</sup>
std dev	full variance-covariance
isotropic convergence <sup>c</sup>	$R_1 = 13.8\%$ , $R_2 = 15.2\%$
isotropic-anisotropic convergence	$R_1 = 10.1\%$ , $R_2 = 11.8\%$
max shifts ( $\Delta/\sigma$ )	1
data/parameters	8150/581
max resid intns of final diff map, c/Å <sup>3</sup>	0.98

<sup>a</sup>The raw intensity is given as  $I_{raw} = (20.116 \times ATN)(C - RB)/NPI$ , here *C* is total counts, *R* is the ratio of scan time to background counting time, *B* is total background counts, *NPI* is the ratio of fastest possible scan rate to scan rate for the measurement, and *ATN* is the attenuator factor (10.7 for Mo in our case). And the observed structure factor amplitude is obtained as the square root of the intensity after correction for Lorentz-polarization:  $F_o = (I_{raw}/Lp)^{1/2}$ . <sup>b</sup>All least-squares refinements were based on the minimization of  $\sum w_i |F_o| - |F_c|$  with the individual weights  $w_i = 1/\sigma_i^2(F_o)$ . Atomic scattering factors used for all atoms are from Cromer, D. T.; Waber, J. T. *International Tables for X-ray Crystallography*; Thekynoch Press: Birmingham, England, 1974; Vol. IV, Table 2.2B; Cromer, D. T.; Mann, J. B. X-ray Scattering Factors Computed from Numerical Hartree-Fock Wave Functions. *Acta Crystallogr.* **1968**, *A24*, 321–324. <sup>c</sup> $R_1 = [\sum |F_o| - |F_c|]/\sum |F_o| \times 100\%$  and  $R_2 = [\sum w_i |F_o| - |F_c|]/\sum w_i |F_o|^{1/2} \times 100\%$ . See supplementary material for a listing of observed and calculated structure factors.

sahedra sharing a vertex, the 37- and 38-atom clusters as three icosahedra sharing three vertices in a cyclic manner plus one and two capping atoms, respectively.<sup>3,4</sup>

This paper describes the full single-crystal X-ray structure of the 38-atom cluster (*p*-Tol<sub>3</sub>P)<sub>12</sub>Au<sub>18</sub>Ag<sub>20</sub>Cl<sub>14</sub> (1). A communication of this cluster, based on preliminary data, has already appeared.<sup>3b</sup>

It is hoped that the structures of this and related clusters, along with the cluster of clusters (C<sup>2</sup>) electron counting approach recently developed by us,<sup>4</sup> will provide new insights in the design and synthesis of very large metal cluster systems via agglomeration of smaller cluster units. We refer to this modular (or building

block) approach to large clusters as the "cluster of clusters" approach (cf. Chart 1), which is to be contrasted with the "layer by layer" growth of the  $\nu_n$  polyhedral clusters<sup>10–14</sup> (cf. Chart 1).

## (II) Experiments and Solutions

**A. Preparation and Crystallization of Compound 1.** To a mixture of (*p*-Tol)<sub>3</sub>PAuCl (0.1 mmol) and [(*p*-Tol)<sub>3</sub>PAgCl]<sub>4</sub> (0.025 mmol) in 100 mL of ethanol was added a solution of NaBH<sub>4</sub> (0.4 mmol) in 40 mL of absolute ethanol. The solution turned dark red immediately upon addition of the reducing agent. The mixture was allowed to react over a period of 24 h until the completion of the reaction. The solution was then filtered. To the filtrate was added a solution of 0.1 mmol of NaSbF<sub>6</sub> in 10 mL of ethanol. The reaction mixture was allowed to stir for a few more minutes and was then refiltered. The dark brown-red product was recrystallized from ethanol/hexanes (ratio of ethanol/hexanes is approximately 5:1) by evaporation under nitrogen at room temperature (yield 27%). FTIR (Digilab FTS40) indicated the absence of SbF<sub>6</sub><sup>-</sup>.

**B. Collection and Reduction of X-ray Data.** A dark-red prismatic crystal of dimensions 0.1 mm × 0.1 mm × 0.05 mm was selected and mounted in a glass capillary. Single-crystal X-ray diffraction data were collected on a Enraf-Nonius CAD4 diffractometer with use of graphite-monochromatized Mo K $\alpha$  radiation ( $\lambda = 0.7107$  Å). Details of the crystal parameters and data collection are summarized in Table I. The diffraction pattern was relatively weak and did not extend beyond  $2\theta > 46^\circ$ . A complete set of data was collected from three crystals over a period of 1 month. For the four octants with  $2^\circ \leq 2\theta \leq 46^\circ$ , 64 687 reflections were measured, after merging from three parts of collected data (part I, 2–20°, crystal 1; part II, 2–20°, crystal 2; part III, 20–23°, crystal 3). It yielded 14 349 independent reflections with  $I > 1\sigma(I)$  after equivalent reflections were averaged by using the program PAINT of the SDP package. A decay correction (using program CHORT) was made on each part of the collected data. The observed intensities were corrected for Lorentz and polarization effects but not for absorption since the  $\psi$  scan data were collected after the crystals had deteriorated. No extinction correction was made. The centrosymmetric space group *P*-1 (No. 2) was confirmed by successful solution and refinement of the structure. Since the center of the cluster (0.486, 0.179, 0.306) is in a general position (viz., *x*, *y*, *z*; -*x*, -*y*, -*z*), the analysis required the location of 18 Au, 20 Ag, 14 Cl, and 12 (Tol)<sub>3</sub>P groups in an asymmetric unit, or equivalently, two clusters (*Z* = 2) per unit cell.

**C. Solution and Refinement of the Structure. 1. Direct Method and Fourier Syntheses.** The positions of the metal atoms were obtained from direct methods, and the Cl and P atoms were located via Fourier syntheses. The majority of the tolyl carbon atoms were located from subsequent difference Fourier syntheses. The missing tolyl carbon atoms were then inferred from the known geometry and the resulting tolyl groups refined as rigid bodies (see the next section). Least-squares refinements of the metal core (the tolyl carbon atoms were included in the calculations but not refined) gave discrepancy factors of  $R_1 = [\sum |F_o| - |F_c|]/\sum |F_o| \times 100\% = 15.2\%$ ,  $R_2 = [\sum w_i |F_o| - |F_c|]/\sum w_i |F_o|^{1/2} \times 100\% = 18.8\%$  where  $w_i = 1/\sigma_i^2(F_o)$ .

**2. Rigid-Body Refinement of Tollyl Groups.** Rigid-body constraints were applied to all 12 tolyl groups with ring C–C distances of 1.39 Å, C–CH<sub>3</sub> distance of 1.47 Å, and a uniform isotropic temperature factor. Tollyl groups were numbered as TY*i*A, TY*i*B, and TY*i*C for tolyl groups A, B, and C, respectively, of the *i*th phosphine ligand, Pi (*i* = 1–12).

(10) (a) Longoni, G.; Dahl, L., unpublished results; (b) Martinengo, S.; Fumagalli, A.; Bonfichi, R.; Ciani, G.; Sironi, A. *J. Chem. Soc., Chem. Commun.* **1982**, 825. (c) Vidal, J. L.; Schoening, R. C.; Troup, J. M., *Inorg. Chem.* **1981**, *20*, 227. (d) Broach, R. W.; Dahl, L. F.; Longoni, G.; Chini, P.; Schultz, A. J.; Williams, J. M. *Adv. Chem. Ser.* **1978**, No. 167, 93. (e) Jackson, P. F.; Johnson, B. F. G.; Lewis, J.; Nelson, W. J. H.; McPartlin, M. *J. Chem. Soc., Dalton Trans.* **1982**, 2099. (f) Hayward, C. M. T.; Shapley, J. R.; Churchill, M. R.; Bueno, C.; Rheingold, A. L. *J. Am. Chem. Soc.* **1982**, *104*, 7347.

(11) (a) Ceriotti, A.; Demartin, F.; Longoni, G.; Manassero, M.; Marchionna, M.; Piva, G.; Sansoni, M. *Angew. Chem., Int. Ed. Engl.* **1985**, *24*, 697. (b) Longoni, G.; Manassero, M.; Sansoni, M. *J. Am. Chem. Soc.* **1980**, *102*, 3242. (c) Fumagalli, A.; Martinengo, S.; Ciani, G.; Sironi, A. *J. Chem. Soc., Chem. Commun.* **1983**, 453. (d) Boyle, P. D.; Johnson, B. J.; Buehler, A.; Pignolet, L. H. *Inorg. Chem.* **1986**, *25*, 5. (e) Alexander, B. D.; Boyle, P. D.; Johnson, B. J.; Casalnuovo, A. L.; John, S. M.; Muetting, A. M.; Pignolet, L. H. *Inorg. Chem.* **1987**, *26*, 2547. (f) Steggerda, J. J.; Bour, J. J.; van der Velden, J. W. A. *Recl.: J. R. Neth. Chem. Soc.* **1982**, *101*, 164.

(12) Kharas, K.; Dahl, L. *Adv. Chem. Phys.* **1988**, *70*, 1.

(13) (a) Chini, P. *Gazz. Chim. Ital.* **1979**, *109*, 225. (b) Chini, P. *J. Organomet. Chem.* **1980**, *200*, 37. (c) Chini, P.; Longoni, G.; Albano, V. G. *Adv. Organomet. Chem.* **1976**, *14*, 285.

(14) Johnson, B. F. G., Ed. *Transition Metal Clusters*; Wiley-Interscience: Chichester, England, 1980.

**Table II.** Selected Interatomic Distances (Å) and Their Estimated Standard Deviations for Cluster (*p*-Tol<sub>3</sub>P)<sub>12</sub>Au<sub>18</sub>Ag<sub>20</sub>Cl<sub>14</sub><sup>a</sup>

atom 1	atom 2	distance	atom 1	atom 2	distance	atom 1	atom 2	distance	atom 1	atom 2	distance
Au1	Au2	3.08 (1)	Au9	Au15	2.685 (9)	Au16	Ag6	2.88 (1)	Ag8	Cl8	3.13 (4)
Au1	Au7	2.96 (1)	Au9	Ag3	2.89 (1)	Au16	Ag7	2.89 (1)	Ag9	Ag10	2.90 (2)
Au1	Au8	2.92 (1)	Au9	Ag5	3.03 (1)	Au16	Ag8	2.95 (1)	Ag9	Ag11	3.10 (1)
Au1	Au13	2.78 (1)	Au9	Ag15	2.85 (1)	Au16	Ag15	3.09 (1)	Ag9	Ag17	2.83 (2)
Au1	Ag11	2.95 (1)	Au9	P9	2.30 (4)	Au16	Ag16	2.83 (1)	Ag9	Cl9	2.45 (4)
Au1	Ag12	2.95 (1)	Au10	Au15	2.685 (8)	Au16	Ag17	2.82 (1)	Ag9	Cl11	3.03 (4)
Au1	P1	2.41 (6)	Au10	Ag4	3.04 (1)	Au16	Ag18	3.01 (2)	Ag10	Ag12	3.09 (1)
Au2	Au7	2.878 (9)	Au10	Ag6	2.89 (1)	Au17	Au18	2.843 (8)	Ag10	Ag18	2.95 (2)
Au2	Au8	2.934 (9)	Au10	Ag16	2.86 (2)	Au17	Ag7	2.78 (1)	Ag10	Cl10	2.44 (4)
Au2	Au13	2.744 (7)	Au10	P10	2.29 (4)	Au17	Ag8	2.79 (1)	Ag11	Ag12	2.89 (2)
Au2	Ag1	2.98 (1)	Au11	Au17	2.719 (8)	Au17	Ag9	2.75 (1)	Ag11	Ag13	2.91 (2)
Au2	Ag2	2.95 (1)	Au11	Ag7	2.90 (1)	Au17	Ag10	2.80 (1)	Ag11	Cl9	2.47 (4)
Au2	P2	2.38 (4)	Au11	Ag9	3.02 (1)	Au17	Ag17	2.82 (1)	Ag12	Ag14	2.83 (2)
Au3	Au4	3.059 (9)	Au11	Ag17	2.89 (1)	Au17	Ag18	2.80 (1)	Ag12	Cl10	2.44 (4)
Au3	Au9	2.94 (1)	Au11	P11	2.34 (4)	Au18	Ag9	2.89 (1)	Ag12	Cl12	3.14 (3)
Au3	Au10	2.87 (1)	Au12	Au17	2.698 (8)	Au18	Ag10	2.87 (2)	Ag13	Ag15	3.24 (2)
Au3	Au15	2.76 (1)	Au12	Ag8	3.04 (2)	Au18	Ag11	2.88 (1)	Ag13	Ag17	3.22 (1)
Au3	Ag3	2.96 (1)	Au12	Ag10	2.91 (1)	Au18	Ag12	2.91 (2)	Ag13	Cl3	2.73 (4)
Au3	Ag4	2.98 (2)	Au12	Ag18	2.89 (1)	Au18	Ag13	2.86 (1)	Ag13	Cl11	2.55 (4)
Au3	P3	2.47 (4)	Au12	P12	2.31 (4)	Au18	Ag14	3.08 (1)	Ag14	Ag16	3.11 (2)
Au4	Au9	2.880 (9)	Au13	Au14	2.87 (1)	Au18	Ag17	3.08 (1)	Ag14	Ag18	3.19 (1)
Au4	Au10	2.95 (1)	Au13	Au18	2.864 (8)	Au18	Ag18	2.82 (1)	Ag14	Cl4	2.56 (4)
Au4	Au15	2.77 (1)	Au13	Ag1	2.80 (1)	Ag1	Ag2	2.85 (2)	Ag14	Cl12	2.73 (4)
Au4	Ag5	3.00 (2)	Au13	Ag2	2.77 (1)	Ag1	Ag3	3.18 (2)	Ag15	Ag17	3.09 (2)
Au4	Ag6	2.97 (2)	Au13	Ag11	2.79 (1)	Ag1	Ag13	2.86 (1)	Ag15	Cl3	2.63 (3)
Au4	P4	2.36 (4)	Au13	Ag12	2.74 (1)	Ag1	Cl1	2.35 (5)	Ag15	Cl7	2.71 (4)
Au5	Au6	3.10 (1)	Au13	Ag13	2.82 (1)	Ag1	Cl3	3.18 (4)	Ag16	Ag18	3.19 (2)
Au5	Au11	2.934 (9)	Au13	Ag14	2.82 (1)	Ag2	Ag4	3.11 (2)	Ag16	Cl4	2.71 (3)
Au5	Au12	2.90 (1)	Au14	Au15	2.86 (1)	Ag2	Ag14	2.93 (1)	Ag16	Cl8	2.60 (4)
Au5	Au17	2.739 (7)	Au14	Au16	2.86 (1)	Ag2	Cl2	2.42 (4)	Ag17	Cl7	2.56 (5)
Au5	Ag7	2.94 (1)	Au14	Au18	2.83 (1)	Ag3	Ag4	2.87 (2)	Ag17	Cl11	2.70 (3)
Au5	Ag8	2.95 (1)	Au14	Ag1	2.96 (1)	Ag3	Ag15	2.92 (2)	Ag18	Cl8	2.69 (4)
Au5	P5	2.35 (3)	Au14	Ag2	2.89 (1)	Ag3	Cl1	2.50 (4)	Ag18	Cl12	2.51 (4)
Au6	Au11	2.93 (1)	Au14	Ag3	2.88 (2)	Ag4	Ag16	2.86 (1)	Ag19	Cl3	2.53 (4)
Au6	Au12	2.95 (1)	Au14	Ag4	2.90 (2)	Ag4	Cl2	2.51 (3)	Ag19	Cl7	2.59 (4)
Au6	Au17	2.76 (1)	Au14	Ag13	3.07 (1)	Ag4	Cl4	3.18 (4)	Ag19	Cl11	2.66 (5)
Au6	Ag9	2.96 (1)	Au14	Ag14	2.85 (2)	Ag5	Ag6	2.89 (2)	Ag19	Cl13	2.38 (5)
Au6	Ag10	2.93 (1)	Au14	Ag15	2.86 (1)	Ag5	Ag7	3.11 (2)	Ag20	Cl4	2.67 (3)
Au6	P6	2.43 (5)	Au14	Ag16	3.07 (1)	Ag5	Ag15	2.83 (1)	Ag20	Cl8	2.53 (4)
Au7	Au13	2.691 (8)	Au15	Au16	2.86 (1)	Ag5	Cl5	2.53 (3)	Ag20	Cl12	2.65 (4)
Au7	Ag1	3.04 (1)	Au15	Ag3	2.80 (1)	Ag5	Cl7	3.21 (4)	Ag20	Cl14	2.37 (5)
Au7	Ag11	2.88 (1)	Au15	Ag4	2.79 (1)	Ag6	Ag8	3.20 (2)	Ag19	Ag13	3.76 (2)
Au7	Ag13	2.85 (1)	Au15	Ag5	2.76 (1)	Ag6	Ag16	2.92 (1)	Ag19	Ag15	3.70 (2)
Au7	P7	2.31 (4)	Au15	Ag6	2.79 (1)	Ag6	Cl6	2.47 (3)	Ag19	Ag17	3.69 (2)
Au8	Au13	2.706 (8)	Au15	Ag15	2.81 (1)	Ag7	Ag8	2.87 (2)	Ag20	Ag14	3.80 (2)
Au8	Ag2	2.91 (2)	Au15	Ag16	2.82 (1)	Ag7	Ag17	2.89 (1)	Ag20	Ag16	3.69 (2)
Au8	Ag12	3.01 (1)	Au16	Au17	2.86 (1)	Ag7	Cl5	2.44 (5)	Ag20	Ag18	3.76 (2)
Au8	Ag14	2.88 (1)	Au16	Au18	2.82 (1)	Ag8	Ag18	2.86 (1)			
Au8	P8	2.32 (4)	Au16	Ag5	2.91 (2)	Ag8	Cl6	2.39 (4)			

<sup>a</sup>Numbers in parentheses are estimated standard deviations in the least significant digits.

Individual carbons are numbered as *C<sub>imj</sub>* (where *i* = 1–12, *m* = A–C, and *j* = 1–7) for the *C<sub>j</sub>* carbon of the *m*th tolyl group bonded to the *i*th phosphine ligand. The position and orientation of the tolyl groups were refined with the group positional parameters *x*, *y*, *z* (in fractional coordinates) and orientation parameters *φ*, *θ*, *ρ* (in degrees), respectively. The discrepancy factors at this point were *R*<sub>1</sub> = 13.8%, *R*<sub>2</sub> = 15.2%.

**3. Disordered Solvent Atoms.** All solvent molecules, as revealed by difference Fourier syntheses, are highly disordered. The following strategy of least-squares refinements was adopted. First, the occupancy factors of the solvent atoms were refined by using an isotropic thermal parameter of *B* = 8 Å<sup>2</sup> (roughly the average of the tolyl groups). The refined occupancy factors of these atoms were then fixed while their thermal parameters (*B*'s) were being refined along with all heavy atoms (refining positional and thermal parameters) and all tolyl groups (included in the calculations but not refined).

**4. Final Cycles of Refinement.** In the final cycles of the refinement, anisotropic thermal parameters were used for heavy atoms (Au, Ag, Cl, and P) while the highly disordered solvent atoms were refined isotropically. Tolyl atoms, already refined as rigid-body groups as described in 11.C.2, were not refined but included in the calculations. Final *R*<sub>1</sub> =  $[\sum |F_o| - |F_c|] / \sum |F_o| \times 100\%$  and *R*<sub>2</sub> =  $[\sum w_i |F_o| - |F_c|]^2 / \sum w_i |F_o|^2]^{1/2} \times 100\%$  values were 10.1% and 11.8%, respectively, for 8150 unique reflections with *I* > 3σ(*I*) and 581 variables. After a final full-matrix refinement, a difference map showed no peaks > 1.0 electron Å<sup>-3</sup> (except near heavy atoms). Final atomic coordinates and thermal parameters with the estimated standard deviations of cluster **1** (heavy atoms only)

are presented in Table A and Table B (supplementary material), respectively. The final positional and thermal parameters from the output of the last cycle of constrained least-squares refinement of cluster **1** for each group (*x*, *y*, *z*, *φ*, *θ*, *ρ*, and *B*) and for individual tolyl ring-carbon atoms (*x*, *y*, *z*, and *B*) are listed in Table C and Table D (supplementary material), respectively. Also given in Table C are the internal coordinates of the tolyl groups. The results of the positional and thermal parameters with the refined occupancy factors of solvent atoms are summarized in Table E (supplementary material). Selected interatomic distances and bond angles, together with the estimated standard deviations, are given in Tables II and III, respectively. Least-squares calculations of "best" molecular planes formed by certain groups of atoms and the perpendicular distance of these and other atoms from those planes are summarized in Table F (supplementary material). Selected intra- and intermolecular van der Waals contacts are listed in Table G (supplementary material). Observed and calculated structure factors are listed in Table H (supplementary material).

### (III) Results and Discussion

**A. Cluster Architecture.** The [Au<sub>18</sub>Ag<sub>20</sub>] and [P<sub>12</sub>Au<sub>18</sub>Ag<sub>20</sub>Cl<sub>14</sub>] frameworks of cluster **1**, which conform to idealized *D*<sub>3h</sub> symmetry, are portrayed in Figure 1, parts a and b, respectively. The most obvious description of the structure is as three 13-atom (Au<sub>7</sub>Ag<sub>6</sub>) Au-centered icosahedra sharing three Au vertices in a cyclic

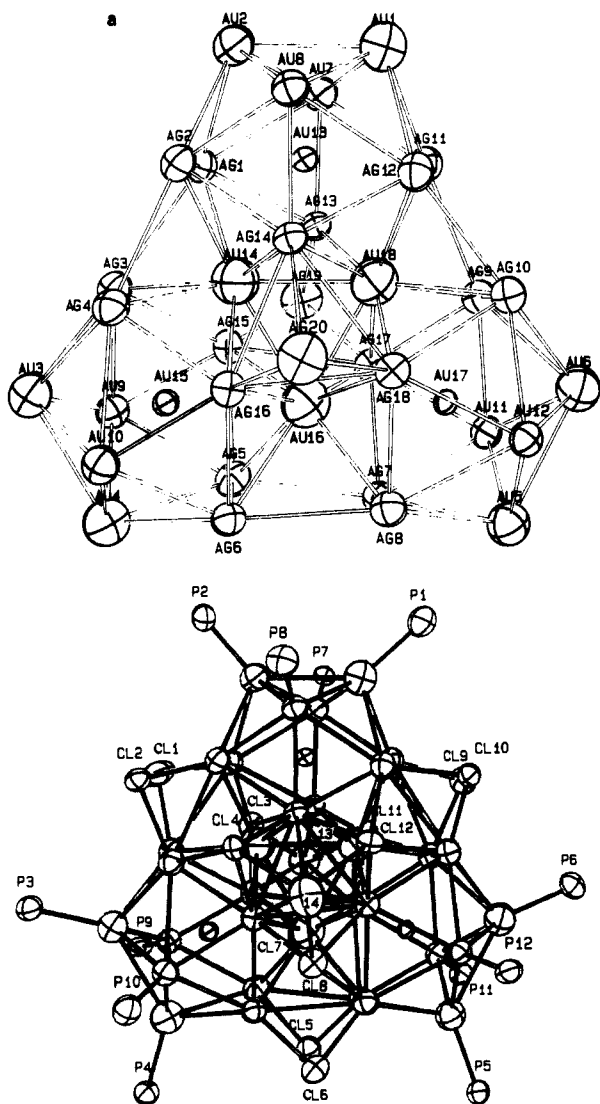


**Figure 1.** (a)  $[\text{Au}_{18}\text{Ag}_{20}]$  framework of cluster 1 depicting three 13-atom ( $\text{Au}_7\text{Ag}_6$ ) Au-centered icosahedra sharing three Au vertices in a cyclic manner plus two capping Ag atoms ( $\text{Ag}_{19}$  and  $\text{Ag}_{20}$ ) located on the idealized 3-fold axis. (b)  $[\text{P}_{12}\text{Au}_{18}\text{Ag}_{20}\text{Cl}_{14}]$  framework of cluster 1. All bonds radiating from the centers of the icosahedra ( $\text{Au}_{13}$ ,  $\text{Au}_{15}$ , and  $\text{Au}_{17}$ ) are omitted for clarity. In (b),  $\text{Cl}_{13}$  and  $\text{Cl}_{14}$  are designated 13 and 14, respectively, for clarity.

manner plus two capping Ag atoms located on the idealized 3-fold axis. As such, the 18 Au atoms can be divided into two categories: 12 on the surface ( $\text{Au}_1$ – $\text{Au}_{12}$ ) and 6 in the interior. The six interior gold atoms include the icosahedral centers  $\text{Au}_3$ ,  $\text{Au}_5$ , and  $\text{Au}_7$  and the shared vertices  $\text{Au}_{14}$ ,  $\text{Au}_{16}$ , and  $\text{Au}_{18}$ . The 20 Ag atoms can be classified into three types (with decreasing distance from the idealized 3-fold symmetry axis of the cluster): 12 on the peripherals (type A  $\text{Ag}_1$ – $\text{Ag}_{12}$ ), 6 in the center (type B  $\text{Ag}_{13}$ – $\text{Ag}_{18}$ ), and 2 on the idealized 3-fold axis (type C  $\text{Ag}_{19}$  and  $\text{Ag}_{20}$ ).

A second description of the metal framework is based on close packing of metal atoms (cf. Figure 2 of ref 3b). In this description, imagine a two-dimensional arrangement of 12 Au atoms, forming a  $\nu_2$  triangle and three  $\nu_1$  triangles sharing corners. Above and below the three small triangles are six Au atoms conceptually changing the smaller triangles into trigonal bipyramids. Above and below the central (large) triangle are eight Ag atoms arranged in two tetrahedral arrays, which are connected by an elongated and distorted trigonal prism. Further addition of three distorted squares of Ag atoms (total of 12) to the three square faces of the distorted trigonal prism completes the arrangement of the 20 Ag atoms in the cluster.

Yet a third description of the structure is that it can be considered as three interpenetrating 25-atom clusters. Thus, if one

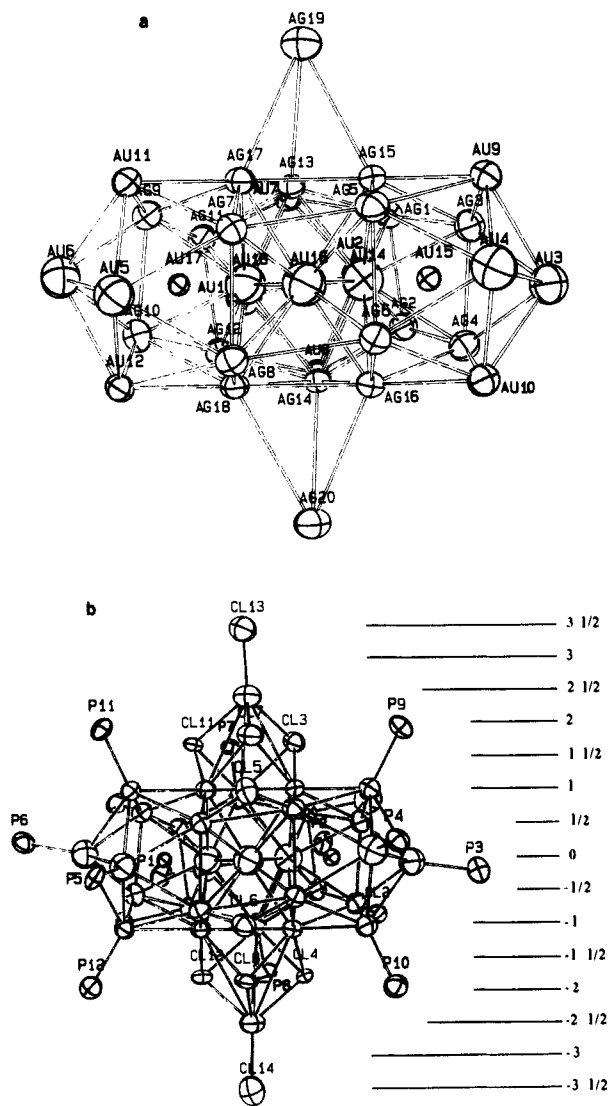


**Figure 2.** Side views of (a) the metal framework  $[\text{Au}_{18}\text{Ag}_{20}]$  and (b) the  $[\text{P}_{12}\text{Au}_{18}\text{Ag}_{20}\text{Cl}_{14}]$  framework of cluster 1. Also shown in (b) is a labeling system for the approximate layers.

views along the pseudo-5-fold axes marked by an arrow in Figure 2 of ref 3b, the same 1:5:1:5:1:5:1:5:1 structural arrangement of metal atoms can be seen. (Note, however, that the four pentagons are arranged in a *s-e-s* configuration in the 25-atom cluster, where *s* and *e* denote staggered and eclipsed, respectively.) The structure is completed by two "apical" Ag atoms located on the idealized 3-fold axis.

The side views of the  $[\text{Au}_{18}\text{Ag}_{20}]$  and the  $[\text{P}_{12}\text{Au}_{18}\text{Ag}_{20}\text{Cl}_{14}]$  frameworks of cluster 1 are portrayed in Figure 2, parts a and b, respectively. A labeling system for the approximate layer arrangement of the heavy atoms is also indicated in Figure 2b.

**B. Cluster Parameters.** Considering the *metal framework* of cluster 1, the 18 Au atoms fall into two distinct classes exhibiting different coordination patterns: the central  $\nu_2$  triangle Au atoms ( $\text{Au}_{13}$ – $\text{Au}_{18}$ ), which are perpendicular to the 3-fold axis, are twelve-coordinate, the peripheral Au atoms, which form a highly distorted twinned cuboctahedron, are six-coordinate. The 20 Ag atoms can also be categorized into three groups in terms of coordination patterns: type A, B, and C Ag atoms are seven-, eight-, and zero-coordinate, respectively (see next paragraph). Here we consider only metal–metal contacts.

The metal–metal distances follow the approximate trend  $\text{Au–Au}$  (2.69–3.09 Å)  $\sim$   $\text{Au–Ag}$  (2.75–3.09 Å)  $<$   $\text{Ag–Ag}$  (2.84–3.24 Å), all of which can be considered as more or less bonding. There are four groups of Ag–Ag distances: 2.83–2.95 Å for unbridged, 3.09–3.20 Å for doubly bridged and 3.09–3.24 Å for triply bridged Ag–Ag bonds. The  $\text{Ag}\cdots\text{Ag}$  contacts of 3.69–3.80 Å involving











Table III (Continued)

atom 1	atom 2	atom 3	angle	atom 1	atom 2	atom 3	angle	atom 1	atom 2	atom 3	angle	atom 1	atom 2	atom 3	angle
Ag14	Ag18	Ag16	58.5 (3)	Cl12	Ag20	Cl14	123 (2)	Ag5	Cl17	Ag15	56.2 (7)	Ag9	Cl11	Ag19	148 (1)
Ag14	Ag18	Cl8	93.5 (8)	Ag1	Cl1	Ag3	82 (1)	Ag5	Cl17	Ag17	82 (1)	Ag13	Cl11	Ag17	76 (1)
Ag14	Ag18	Cl12	55.8 (8)	Ag2	Cl2	Ag4	78 (1)	Ag5	Cl17	Ag19	144 (1)	Ag13	Cl11	Ag19	93 (1)
Ag16	Ag18	Cl8	51.6 (9)	Ag1	Cl3	Ag13	57.4 (8)	Ag15	Cl17	Ag17	72 (1)	Ag17	Cl11	Ag19	90 (1)
Ag16	Ag18	Cl12	95 (1)	Ag1	Cl3	Ag15	87 (1)	Ag15	Cl17	Ag19	89 (1)	Ag12	Cl12	Ag14	57.2 (7)
Cl8	Ag18	Cl12	86 (1)	Ag1	Cl3	Ag19	148 (2)	Ag17	Cl17	Ag19	94 (1)	Ag12	Cl12	Ag18	85 (1)
Cl3	Ag19	Cl7	92 (1)	Ag13	Cl3	Ag15	74 (1)	Ag8	Cl8	Ag16	88 (1)	Ag12	Cl12	Ag20	146 (1)
Cl3	Ag19	Cl11	89 (1)	Ag13	Cl3	Ag19	91 (1)	Ag8	Cl8	Ag18	58.3 (7)	Ag14	Cl12	Ag18	75 (1)
Cl3	Ag19	Cl13	128 (1)	Ag15	Cl3	Ag19	92 (1)	Ag8	Cl8	Ag20	149 (2)	Ag14	Cl12	Ag20	90 (1)
Cl7	Ag19	Cl11	87 (1)	Ag4	Cl4	Ag14	83.7 (9)	Ag16	Cl8	Ag18	74 (1)	Ag18	Cl12	Ag20	94 (1)
Cl7	Ag19	Cl13	126 (1)	Ag4	Cl4	Ag16	57.5 (7)	Ag16	Cl8	Ag20	92 (1)	Ag13	Ag19	Ag15	51.5 (3)
Cl11	Ag19	Cl13	123 (2)	Ag4	Cl4	Ag20	143 (1)	Ag18	Cl8	Ag20	92 (1)	Ag13	Ag19	Ag17	50.5 (3)
Cl4	Ag20	Cl8	92 (1)	Ag14	Cl4	Ag16	72.3 (8)	Ag9	Cl9	Ag11	78 (1)	Ag15	Ag19	Ag17	48.8 (3)
Cl4	Ag20	Cl12	87 (1)	Ag14	Cl4	Ag20	93 (1)	Ag10	Cl10	Ag12	79 (1)	Ag14	Ag20	Ag16	49.0 (3)
Cl4	Ag20	Cl14	125 (1)	Ag16	Cl4	Ag20	86.8 (8)	Ag9	Cl11	Ag13	86 (1)	Ag14	Ag20	Ag18	49.8 (3)
Cl8	Ag20	Cl12	87 (1)	Ag5	Cl5	Ag7	78 (1)	Ag9	Cl11	Ag17	58.8 (8)	Ag16	Ag20	Ag18	50.6 (3)
Cl8	Ag20	Cl14	130 (1)	Ag6	Cl6	Ag8	82.3 (9)								

\*Numbers in parentheses are estimated standard deviations in the least significant digits.

the apical Ag atoms are best considered as nonbonding.

The terminal, doubly, and triply bridging Ag-Cl distances fall in the range of 2.37–2.38, 2.35–2.53, and 2.51–2.73 Å, with an average of 2.37, 2.44, and 2.62 Å, respectively. The 12 Au-P distances fall in the range of 2.29–2.47 Å, with an average of 2.38 Å.

**C. 13-Atom Icosahedral Cluster Units.** The basic building block of the 38-atom cluster is the 13-atom centered icosahedral unit. An icosahedron has 12 vertices, 20 triangular faces, and 30 edges. A hole is created that is capable of housing an additional "interior atom" of roughly 10% smaller in size than the "surface atoms". Thus, the metal-metal distances involving the three centroids of the three icosahedra (Au13, Au15, and Au17) are among the shortest (~2.74 Å) in the cluster 1.

The idealized icosahedron belongs to the  $I_h$  point group, which has an inversion symmetry. Therefore, it should have six linear arrays of metal atoms. Indeed, each of the center atoms, Au13, Au15, and Au17, has six M-M-M bond angles (M = Au or Ag) close to linearity (>170°) (cf. Table III).

The spread of the distances around the icosahedral central atoms (for example, the distances of central Au13 to peripheral Au or Ag atoms range from 2.69 (1) Å for the Au13-Au7 bond to 2.87 (1) Å for the Au13-Au14 bond) indicates slight distortions of icosahedral unit away from the idealized icosahedral geometry and in large measure can be attributed to the distribution of different kinds of gold and silver atoms, and bonding and/or steric effects imposed by the (ToI)<sub>3</sub>P and the chlorine ligands.

If we focus our attention on the surface of an icosahedron, each of the 12 vertices is common to 5 triangular faces and 5 pentagonal cross sections. Thus the M-M-M angles on the surface of an ideal icosahedron must either be 60° or 108°. Indeed, Table III shows that all peripheral M-M-M (M = Au or Ag) angles in cluster 1 lie in the range of either 55.5–67.8° or 103.7–123.7° within each icosahedral unit.

**D. 13-Atom Bicapped Pentagonal Prisms.** The three shared vertices, Au14, Au16, and Au18, can be considered as centroids of three 13-atom bicapped pentagonal prisms.

A bicapped pentagonal prism belongs to  $D_{5h}$  symmetry with 12 vertices, 15 faces (10 triangles and 5 squares), and 25 edges. Since it does not have an inversion symmetry, there is only one linear array of three metal atoms. This is exactly what is observed: for example, only the bond angle of Au13-Au14-Au15 of 178.6 (4)° is close to linearity; all other angles centered around Au14 are 158° or smaller.

Unlike icosahedra, which have only triangular faces, bicapped pentagonal prisms have five square faces. This is indeed observed. For example, the four internal angles of the Ag1-Ag2-Ag4-Ag3 square are 99.4 (5)°, 81.1 (4)°, 97.4 (5)°, and 80.2 (4)°, with an average of 90°. Even the "squares" involving the shared vertices are not far from right angles; for example, the angles for Ag14-Ag16-Au16-Au18 (with the latter two atoms as shared vertices) are 89.1 (4)°, 95.5 (4)°, 90.0 (4)°, and 84.9 (4)°, again, with an average of 90°.

**E. Nearly Close Packed Layers.** Referring to Figure 2b, the 18 Au atoms are distributed approximately in three layers: 12 in the central layer denoted as the 0th layer and three each in layers ±1. The six central (type B) Ag atoms also lie in layers ±1. The 12 peripheral (type A) Ag atoms lie approximately halfway between layer 0 and layers ±1, which we shall call layers ±1/2. Finally, the two exo-cluster apical (type C) Ag atoms are located in layers ±2 1/2. Note that the two apical (type C) Ag atoms are located in layers ±2 1/2 rather than ±2 because they are more distant from the cluster mainframe (cf. section III.B).

**F. Terminal, Doubly, and Triply Bridging Halides.** The 14 chloride ligands coordinate exclusively to the 20 Ag atoms. They are of three distinct types: six doubly bridging  $\mu_2$ -Cl (connecting type A Ag atoms of adjacent icosahedra); six triply bridging  $\mu_3$ -Cl (connecting type B and type C Ag atoms); and two terminal Cl (coordinated to type C Ag atoms). The coexistence of all three modes of bridging for the halide ligands in one cluster is rather interesting.

All Ag-Cl distances are normal. The averages (range in parentheses) of terminal, doubly, and triply bridging Ag-Cl distances are 2.37 (2.37–2.38), 2.44 (2.35–2.53), and 2.62 (2.51–2.73) Å, respectively.

One interesting observation is that the triply bridging chloride ligands have short Cl...Ag contacts of ca. 3.1 Å (e.g., Cl8...Ag8), which is significantly less than the sum (3.55 Å) of van der Waals radius of Cl (1.80 Å) and the atomic radius of Ag (1.75 Å). Though these distances are too long to be considered as normal covalent bonds, the tendency toward a quadruply bridging ( $\mu_4$ ) mode is noteworthy. It should be cautioned that this may be a manifestation of the tendency toward a more-or-less close packing of the chloride ligands over the silver layers.

The disposition of the 14 chloride ligands can be described as two nonbonding tetrahedra linked by three bridges. Alternatively, it can be described as a twisted trigonal prism (triply bridging halides Cl3, Cl4, Cl7, Cl8, Cl11, Cl12) with two triangular face caps (terminal halides Cl13 and Cl14). Concentric with this trigonal prism is another twisted trigonal prism (doubly bridging ligands Cl1, Cl2, Cl5, Cl6, Cl9, Cl10), which is shorter in height but larger in base area. Selected Cl...Cl contacts are tabulated in Table IV.

As shown in Figure 2b, the six doubly bridging chlorides are situated approximately in layers ±1 whereas the six triply bridging chlorides lie roughly in layers ±2. The terminal chlorides lie roughly in layers ±3 1/2.

**G. The Twelve Phosphines.** Globally, the 12 tri(*p*-tolyl)-phosphine ligands, which coordinate to 12 peripheral Au atoms in a radial fashion (viz., away from the centered Au atoms of the three icosahedra), form a highly distorted twinned cuboctahedron. The nonbonding P...P distances are provided in Table V. Here, however, the central triangles of the distorted twinned cuboctahedron are enlarged since the phosphines are attached to the peripheral gold atoms only.

It is observed that the P atoms of six of the phosphine ligands

**Table IV.** Selected Nonbonding Cl...Cl Distances in the Cluster (*p*-Tol<sub>3</sub>P)<sub>12</sub>Au<sub>18</sub>Ag<sub>20</sub>Cl<sub>14</sub><sup>a</sup>

atom 1	atom 2	distance	atom 1	atom 2	distance
Cl1	Cl2	4.16 (5)	Cl6	Cl8	3.71 (5)
Cl1	Cl3	3.76 (5)	Cl7	Cl11	3.61 (5)
Cl2	Cl4	3.88 (4)	Cl7	Cl13	4.43 (5)
Cl3	Cl7	3.66 (4)	Cl8	Cl12	3.56 (5)
Cl3	Cl11	3.60 (5)	Cl8	Cl14	4.43 (5)
Cl3	Cl13	4.42 (5)	Cl9	Cl10	4.31 (5)
Cl4	Cl8	3.70 (3)	Cl9	Cl11	3.84 (6)
Cl4	Cl12	3.65 (5)	Cl10	Cl12	3.81 (5)
Cl4	Cl14	4.47 (5)	Cl11	Cl13	4.43 (5)
Cl5	Cl6	4.26 (5)	Cl12	Cl14	4.41 (5)
Cl5	Cl7	3.87 (4)			

<sup>a</sup>Numbers in parentheses are estimated standard deviations in the least significant digits.

**Table V.** Selected Nonbonding P...P Distances in the Cluster (*p*-Tol<sub>3</sub>P)<sub>12</sub>Au<sub>18</sub>Ag<sub>20</sub>Cl<sub>14</sub><sup>a</sup>

atom 1	atom 2	distance	atom 1	atom 2	distance
P1	P2	6.43 (6)	P4	P9	5.46 (4)
P1	P6	8.88 (4)	P4	P10	5.64 (5)
P1	P7	5.72 (6)	P5	P6	6.57 (5)
P1	P8	5.58 (6)	P5	P11	5.60 (5)
P2	P3	9.75 (6)	P5	P12	5.36 (5)
P2	P7	5.34 (5)	P6	P11	5.56 (6)
P2	P8	5.61 (5)	P6	P12	5.77 (5)
P3	P4	6.41 (4)	P7	P8	8.63 (5)
P3	P9	5.76 (5)	P9	P10	8.62 (5)
P3	P10	5.44 (5)	P11	P12	8.61 (5)
P4	P5	9.64 (5)			

<sup>a</sup>Numbers in parentheses are estimated standard deviations in the least significant digits.

(hereafter referred to as "equatorial" ligands) are roughly coplanar with the center layer of 12 Au atoms. Deviations of the P atoms from the least-squares planes of the Au atoms are tabulated in Table F (supplementary material). The remaining six P atoms (hereafter referred to as "axial" ligands), three above and three below the Au plane, lie approximately in layers  $\pm 2$ . The six equatorial P atoms are twisted slightly (viz., not exactly coplanar) giving rise to a "chair" conformation; these atoms, however, are roughly equidistant from the plane of the 12 central Au atoms [cf. Table F (supplementary material)].

If we focus our attention on the individual icosahedron, we see that the four peripheral Au atoms, for example, Au1, Au2, Au7, Au8, along with the central atom Au13, form a trigonal bipyramid. The four phosphine ligands are coordinated to the four peripheral Au atoms as follows: P1 and P2 (coordinated to Au1 and Au2) occupy the equatorial positions while P7 and P8 (coordinated to Au7 and Au8) occupy the axial positions.

The 12 phosphine ligands can be divided into two classes in terms of bond lengths and angles. The difference of bond lengths between the two kinds of phosphine ligands is reflected in (cf. Table II) the shorter Au-P(axial) bond lengths (in the range of 2.29–2.34 Å, with an average of 2.31 Å) compared to the Au-P(equatorial) bond lengths (2.35–2.47 Å, with an average of 2.40 Å). All the Au(central)-Au(peripheral)-P moieties are essentially linear, although the degree of their slight bending is significant enough to tell the difference between equatorial and axial phosphines. The Au(central)-Au(peripheral)-P(equatorial) angles span the range of 161.7–171.0°. These values deviate significantly from linearity. The corresponding Au(central)-Au(peripheral)-P(axial) angles deviate less from linearity, which lies in the range of 177–179.3°. We believe that the larger deviation of the Au-Au-P angles from linearity and the longer Au-P bond lengths for the equatorial phosphines are manifestations of steric repulsions between adjacent phosphine ligands in the equatorial plane.

The 36 Au-P-C angles, ranging from 110° to 125° (with a few exceptions), are greater than the ideal tetrahedral angle whereas the 36 C-P-C angles, ranging from 100° to 115°, are significantly smaller (cf. Table VII). An interesting pattern is also observed for the P-C-C (cf. Table VII): viz., those oriented

**Table VI.** P-C(tolyl) Distances in the Cluster (*p*-Tol<sub>3</sub>P)<sub>12</sub>Au<sub>18</sub>Ag<sub>20</sub>Cl<sub>14</sub><sup>a</sup>

atom 1	atom 2	distance	atom 1	atom 2	distance
P1	C1C1	1.62 (4)	P7	C7A1	1.60 (3)
P1	C1A1	1.83 (5)	P7	C7B1	1.76 (4)
P1	C1B1	1.81 (5)	P7	C7C1	1.97 (4)
P2	C2A1	1.82 (5)	P8	C8A1	1.87 (4)
P2	C2B1	1.78 (5)	P8	C8C1	1.67 (5)
P2	C2C1	1.84 (5)	P8	C8B1	1.82 (4)
P3	C3C1	1.54 (5)	P9	C9A1	1.68 (5)
P3	C3A1	1.66 (4)	P9	C9C1	1.95 (3)
P3	C3B1	1.67 (4)	P9	C9B1	1.78 (4)
P4	C4A1	1.72 (4)	P10	C10A1	1.74 (5)
P4	C4B1	1.57 (5)	P10	C10B1	1.90 (3)
P4	C4C1	1.85 (4)	P10	C10C1	1.79 (4)
P5	C5C1	1.65 (4)	P11	C11B1	1.90 (4)
P5	C5A1	1.85 (4)	P11	C11A1	1.69 (5)
P5	C5B1	1.71 (4)	P11	C11C1	1.83 (4)
P6	C6C1	1.88 (4)	P12	C12A1	1.88 (4)
P6	C6B1	1.65 (4)	P12	C12B1	1.79 (4)
P6	C6A1	1.86 (4)	P12	C12C1	1.46 (4)

<sup>a</sup>Numbers in parentheses are estimated standard deviations in the least significant digits.

toward the pseudo-3-fold axis of the (Tol)<sub>3</sub>P are all greater than the ideal trigonal angle of 120° whereas those oriented in the opposite direction are somewhat smaller. These observations for cluster **1** are very similar to those observed in the cubane-like (Ph<sub>3</sub>P)<sub>4</sub>M<sub>4</sub>X<sub>4</sub> (M = Cu, Ag; and X = Cl, Br, I).<sup>15</sup>

**H. Highly Disordered Solvent Molecules.** Since large metal clusters of interest here are beginning to approach the size of small proteins, it is not surprising that X-ray structural determination of these large "small" molecules carries the same problems often encountered in the small "large" molecules of proteins. The solvent molecules are highly disordered and/or lost during data collection as a result of crystal decay. Consequently, only 125 atoms with electron densities greater than 1.0 e/Å<sup>3</sup> were found in the difference Fourier map. In some cases, solvents are associated by hydrogen bonding or weak O-H...Cl (or C-H...Cl) or weak O-H...C<sub>ring</sub> (or C-H...C<sub>ring</sub>) interactions with cluster **1**. Interatomic distances corresponding to shorter than normal van der Waals contacts of cluster **1** and solvents (O-H...Cl or C-H...Cl  $\geq 2.8$  and  $\leq 3.8$  Å, and O-H...C<sub>ring</sub> or C-H...C<sub>ring</sub>  $\geq 2.6$  and  $\leq 3.4$  Å) are summarized in Table G (supplementary material). The formula, therefore, is approximately 1.42EtOH. However, not all of these solvent molecules are of unit weight. Some are lost during data collection; some are smeared out due to disorder and/or liquidlike arrangement. As described previously, such disorder was modeled by first refining the occupancy of the solvent atoms with a fixed isotropic temperature factor of 8 Å<sup>2</sup> (roughly the average of the tolyl groups), followed by refining the isotropic thermal parameter while holding the occupancy fixed. By adding up the occupancies (weight), a total of 37 EtOH molecules per asymmetric unit can be obtained. The final formula for the crystal with which the data were collected, therefore, is approximately 1.37EtOH. Owing to the highly disordered nature of the solvent molecules, no attempts were made to interpret their bond lengths and angles.

**I. Empirical Structural Rules for the Au-Ag Supraclusters.** A close examination of the structure of cluster **1** and related clusters revealed that there are certain empirical rules in the formation of these clusters: (1) the halide ligands are bonded to the silver atoms; (2) the phosphine ligands are attached to the gold atoms; (3) the "interstitial" or "bulk" atom in the icosahedral cages are gold atoms; and (4) the "shared" vertices (bicapped pentagonal prismatic cages) are also gold atoms.

These rules may explain why the structures of this class of Au-Ag clusters are ordered (rather than a statistical distribution of Au and Ag atoms within the metal framework) despite the fact that Au and Ag are roughly equal in size and completely miscible in the alloy solid solution.

(15) Teo, B. K.; Calabrese, J. C. *Inorg. Chem.* 1976, 15, 2467.

Table VII. Au-P-C, C-P-C, and P-C-C Angles in the Cluster (*p*-Tol<sub>3</sub>P)<sub>12</sub>Au<sub>18</sub>Ag<sub>20</sub>Cl<sub>14</sub><sup>a</sup>

atom 1	atom 2	atom 3	angle	atom 1	atom 2	atom 3	angle	atom 1	atom 2	atom 3	angle	atom 1	atom 2	atom 3	angle
Au1	P1	C1C1	125 (3)	Au4	P4	C4A1	110 (2)	Au7	P7	C7A1	117 (2)	Au10	P10	C10A1	115 (2)
Au1	P1	C1A1	104 (2)	Au4	P4	C4B1	117 (2)	Au7	P7	C7B1	111 (2)	Au10	P10	C10B1	110 (2)
Au1	P1	C1B1	110 (2)	Au4	P4	C4C1	103 (2)	Au7	P7	C7C1	115 (1)	Au10	P10	C10C1	110 (2)
C1C1	P1	C1A1	103 (3)	C4A1	P4	C4B1	100 (2)	C7A1	P7	C7B1	102 (2)	C10A1	P10	C10B1	100 (2)
C1C1	P1	C1B1	105 (3)	C4A1	P4	C4C1	115 (2)	C7A1	P7	C7C1	102 (2)	C10A1	P10	C10C1	104 (2)
C1A1	P1	C1B1	108 (2)	C4B1	P4	C4C1	113 (2)	C7B1	P7	C7C1	108 (2)	C10B1	P10	C10C1	117 (2)
Au2	P2	C2A1	110 (2)	Au5	P5	C5C1	99 (2)	Au8	P8	C8A1	115 (2)	Au11	P11	C11B1	112 (2)
Au2	P2	C2B1	117 (2)	Au5	P5	C5A1	116 (2)	Au8	P8	C8C1	110 (3)	Au11	P11	C11A1	109 (2)
Au2	P2	C2C1	112 (2)	Au5	P5	C5B1	116 (2)	Au8	P8	C8B1	112 (2)	Au11	P11	C11C1	116 (2)
C2A1	P2	C2B1	105 (2)	C5C1	P5	C5A1	111 (2)	C8A1	P8	C8C1	107 (2)	C11B1	P11	C11A1	110 (2)
C2A1	P2	C2C1	109 (3)	C5C1	P5	C5B1	109 (2)	C8A1	P8	C8B1	105 (3)	C11B1	P11	C11C1	102 (2)
C2B1	P2	C2C1	103 (2)	C5A1	P5	C5B1	106 (2)	C8C1	P8	C8B1	109 (2)	C11A1	P11	C11C1	107 (2)
Au3	P3	C3C1	113 (2)	Au6	P6	C6C1	123 (2)	Au9	P9	C9A1	116 (2)	Au12	P12	C12A1	115 (2)
Au3	P3	C3A1	108 (2)	Au6	P6	C6B1	113 (2)	Au9	P9	C9C1	115 (2)	Au12	P12	C12B1	112 (2)
Au3	P3	C3B1	109 (2)	Au6	P6	C6A1	101 (2)	Au9	P9	C9B1	111 (2)	Au12	P12	C12C1	112 (2)
C3C1	P3	C3A1	107 (3)	C6C1	P6	C6B1	104 (2)	C9A1	P9	C9C1	104 (2)	C12A1	P12	C12B1	101 (2)
C3C1	P3	C3B1	113 (3)	C6C1	P6	C6A1	103 (2)	C9A1	P9	C9B1	106 (2)	C12A1	P12	C12C1	100 (2)
C3A1	P3	C3B1	108 (2)	C6B1	P6	C6A1	112 (2)	C9C1	P9	C9B1	104 (2)	C12B1	P12	C12C1	116 (2)
P1	C1C1	C1C2	113 (2)	P4	C4C1	C4C2	106 (1)	P7	C7C1	C7C2	112 (1)	P10	C10B1	C10B2	129 (2)
P1	C1A1	C1A6	117 (2)	P4	C4C1	C4C6	134 (1)	P7	C7C1	C7C6	127.7 (9)	P10	C10B1	C10B6	108 (2)
P1	C1B1	C1B2	118 (2)	P5	C5A1	C5A2	126 (1)	P8	C8C1	C8C2	113 (2)	P11	C11C1	C11C2	127 (1)
P2	C2B1	C2B6	117 (1)	P5	C5A1	C5A6	113 (1)	P8	C8C1	C8C6	127 (2)	P11	C11C1	C11C6	113 (1)
P2	C2A1	C2A2	124 (1)	P5	C5B1	C5B2	117 (1)	P8	C8A1	C8A2	123 (2)	P11	C11A1	C11A2	108 (1)
P2	C2A1	C2A6	116 (1)	P5	C5B1	C5B6	123 (1)	P8	C8A1	C8A6	117 (2)	P11	C11A1	C11A6	132 (1)
P2	C2C1	C2C2	130 (2)	P5	C5C1	C5C2	115 (1)	P8	C8B1	C8B2	122 (1)	P9	C9C1	C9C6	124 (1)
P2	C2C1	C2C6	110 (2)	P5	C5C1	C5C6	124 (1)	P8	C8B1	C8B6	118 (1)	P9	C9A1	C9A2	116 (1)
P3	C3C1	C3C2	120 (1)	P6	C6B1	C6B2	109 (2)	P9	C9C1	C9C2	116 (1)	P9	C9A1	C9A6	124 (1)
P3	C3C1	C3C6	118 (1)	P6	C6B1	C6B6	130 (2)	P6	C6C1	C6C2	123 (1)	P9	C9B1	C9B2	122 (1)
P3	C3A1	C3A2	125 (1)	P6	C6A1	C6A2	118 (1)	P6	C6C1	C6C6	117 (1)	P12	C12C1	C12C2	116 (2)
P3	C3A1	C3A6	115 (1)	P6	C6A1	C6A6	122 (1)	P7	C7B1	C7B2	123 (1)	P12	C12C1	C12C6	124 (2)
P3	C3B1	C3B2	116 (2)	P4	C4A1	C4A2	122 (2)	P7	C7B1	C7B6	117 (1)	P11	C11B1	C11B2	120 (1)
P3	C3B1	C3B6	124 (2)	P4	C4A1	C4A6	118 (2)	P9	C9B1	C9B6	117 (1)	P11	C11B1	C11B6	118 (1)
P1	C1C1	C1C6	127 (2)	P4	C4B1	C4B2	112 (1)	P10	C10A1	C10A2	122 (1)	P12	C12A1	C12A2	118 (1)
P1	C1A1	C1A2	123 (2)	P4	C4B1	C4B6	127 (1)	P10	C10A1	C10A6	117 (1)	P12	C12A1	C12A6	122 (1)
P1	C1B1	C1B6	122 (2)	P7	C7A1	C7A2	114 (1)	P10	C10C1	C10C2	121 (1)	P12	C12B1	C12B2	127 (1)
P2	C2B1	C2B2	123 (1)	P7	C7A1	C7A6	125 (1)	P10	C10C1	C10C6	119 (1)	P12	C12B1	C12B6	113 (1)

<sup>a</sup>Numbers in parentheses are estimated standard deviations in the least significant digits.

**J. Crystal Structure.** The crystal structure of the title compound is composed of two cluster **1** and 84 highly disordered, liquidlike EtOH molecules per unit cell. Since the space group is *P*-1, the crystallographically independent asymmetric unit comprises 1.42EtOH.

The centroid of cluster **1** resides at (0.486, 0.179, 0.306) with the idealized 3-fold axis (the Ag19–Ag20 vector) lying approximately parallel to the crystallographic *a* axis. As a result, the central layer (layer 0) of the cluster lies close to *x* = 0.48 plane. Furthermore, the Au13–Au14–Au15 edge of the central  $\nu_2$  gold triangle is nearly parallel to the crystallographic *b* axis. Finally, it is interesting to point out that the coordinates of Ag19 and Ag20 differ only in  $\Delta x \approx 0.5$ .

**K. Electron Counting.** We recently proposed a cluster of clusters (C<sup>2</sup>) model for the electron counting of supraclusters based on vertex-, edge-, or face-sharing of smaller cluster units as building blocks.<sup>4</sup>

The title cluster **1** can be considered as a 36-atom cluster, formed by three 13-atom icosahedra sharing three vertices in a cyclic manner, plus two exopolyhedral Ag atoms. By use of the C<sup>2</sup> approach, the number of skeletal electron pairs for the 36-atom cluster mainframe is  $B = (3 \times 13)$  (three icosahedra) –  $(3 \times 3)$  (sharing three vertices) = 30. Since the number of "surface atoms" is  $V_m = 36 - 3$  (three centroids) = 33, the total number of electron pairs is  $T = 6V_m + B = 6 \times 33 + 30 = 228$ . Since the two exopolyhedral Ag atoms (Ag19 and Ag20) do not form metal-metal bonds with the 36-atom polyhedral framework (Ag...Ag distances ranging from 3.69 to 3.80 Å with an average of 3.73 Å), one can consider that each of these two Ag atoms contributes nine electron pairs (viz., 18 electrons satisfying the effective atom number rule) to the cluster bonding. Thus the total number of electron pairs for the 38-atom cluster **1** will be  $T = 228 + (2 \times 9) = 246$ . The predicted electron count is  $N = 2T = 2 \times 246 = 492$ . This is in good agreement with the observed electron count of  $N_{\text{obs}} = (12 \times 2)$  (phosphine) +  $(38 \times 11)$  (metal) +  $(2 \times 1)$

(terminal Cl) +  $(6 \times 3)$  (doubly bridging Cl) +  $(6 \times 5)$  (triply bridging Cl) = 492.

It is tempting to predict that if one or both of the exopolyhedral Ag atoms begin to form three or six metal-metal bonds with the polyhedral cluster framework, the electron counts will become  $N = 492 - (3 \times 2) = 486$  and  $N = 492 - (6 \times 2) = 480$ , respectively.

**Acknowledgment** is made to the National Science Foundation (CHE-8722339), and the donors of the Petroleum Research Fund, administered by the American Chemical Society, for financial support of this research. We are also grateful to the University of Illinois at Chicago for a Campus Research Board Award. We would also like to express our sincere gratitude to Professor C. Strouse of UCLA for generously providing the rigid-body program and making helpful suggestions for the modification of the crystallographic programs, and to Drs A. Syed, K. Fay, and G. Williams of Enraf-Nonius for their generous help in the modification of the SDP programs.

**Registry No.** **1**, 114654-93-2; 1.42EtOH, 129647-93-4; (*p*-Tol)<sub>3</sub>PAuCl, 28978-10-1; [(*p*-Tol)<sub>3</sub>PAgCl]<sub>4</sub>, 129467-07-8.

**Supplementary Material Available:** Full listings for (*p*-Tol)<sub>3</sub>P)<sub>12</sub>Au<sub>18</sub>Ag<sub>20</sub>Cl<sub>14</sub> of positional parameters and equivalent isotropic thermal parameters (Table A), anisotropic thermal parameters (Table B), positional and orientational parameters of the tolyl groups (Table C), positional and isotropic thermal parameters of individual carbon atoms in the tolyl groups (Table D), atomic positional parameters and equivalent isotropic displacement parameters of solvent atoms (Table E), least-squares planes and distances from the planes of selected groups of atoms (Table F), and selected intra- and intermolecular van der Waals contacts (Table G) (27 pages); listing of observed and calculated structure factors (Table H) for (*p*-Tol)<sub>3</sub>P)<sub>12</sub>Au<sub>18</sub>Ag<sub>20</sub>Cl<sub>14</sub>·42EtOH (47 pages). Ordering information is given on any current masthead page.